PHYSICAL REVIEW B VOLUME 27, NUMBER 4 15 FEBRUARY 1983

Theory of bonding of transition metals to nontransition metals

C. D. Gelatt, Jr., A. R. Williams, and V. L. Moruzzi
IBM Thomas J. Watson Research Center, Yorktown Heights, New York 10598
(Received 1 March 1982; revised manuscript received 29 October 1982)

We present a theory of the chemical bond in compounds consisting of both transition metals and nontransition metals. Chemical trends in the bonding properties are established by directly comparing the total energies of a large number of such compounds with the total energies of their constituents. These chemical trends are analyzed in terms of the *s*-, *p*-, and *d*-like state densities of the compounds and the constituents. Rather different types of bonding are shown to result when the atomic *s* and *p* levels of the nontransition metal lie above, below, and near the energy of the transition-metal *d* level. The heat of compound formation is shown to result from a competition between two simple physical effects: (1) the weakening of the transition-metal bonds by the lattice dilatation required for the accommodation of the nontransition metal, and (2) the increased bonding which results from the occupation of the bonding members of the hybrid states formed from the interaction between the transition-metal *d* states and the *s-p* states on the nontransition metal. Our theoretical values for the heats of formation of these compounds are generally similar to those given by Miedema's empirical formula. Distinctive aspects of the variation of the heat of formation with the number of valence electrons reveal, however, that the microscopic picture on which the empirical formula is based is quite different from that given by our self-consistent energy-band theory.

I. INTRODUCTION

Compounds formed between transition metals and elements with only *s* and *p* electrons in their valence shells (such as the elements lithium through fluorine and sodium through chlorine) display interesting magnetic, superconducting, mechanical, and structural properties. In this paper we present both a microscopic picture of the electronic structure of these compounds and the chemical trends of the bonding that this electronic structure implies.

Both the bonding trends and their microscopic analysis are obtained from theoretical calculations. To make the interpretation of bonding as unambiguous as possible, we avoid in the present study the complications associated with magnetic order and those associated with relativistic effects. We therefore concentrate here on compounds involving the 4*d* transition metals. Calculations for compounds formed from the 4*d* transition metals and the *s-p* elements from the Li and Na rows have been completed.

There have been a number of previous studies of the electronic structure of particular members of the general class of transition-metal—light-element systems. Examples of these are the calculations of Ern and Switendick[1] for the NaCl structure compounds TiC, TiN, and TiO (the first full calculations of the electronic structure of compounds), the work of Neckel *et al.*[2] that extended the study to self-consistent calculations of the compounds formed between the group Sc, Ti, and V and the group C, N, and O, and the study of the electronic structure and equilibrium density of 3*d* monoxides by Andersen *et al.*[3] The present work is distinguished from these studies both by its breadth and by the inclusion of detailed calculations of the energetics of compound formation, the calculation of the heat of formation of the compounds.

Our work is based on parameter-free self-consistent local-density calculations of the electronic structure. The particular implementation is the augmented-spherical-wave method[4] which provides a computationally efficient method of calculating the self-consistent-field charge and state densities as well as the local-density total energy. The only inputs to a particular calculation are the nuclear charges of the constituents and the crystal structure. The solution of the self-consistent-field calculation then yields reliable charge densities from which a charge transfer can be determined. From the total energy per unit cell the equilibrium atomic density is determined by energy minimization.

II. ELECTRONIC STRUCTURE

By studying the electronic density of states decomposed according to site and angular momen-

tum one can distinguish between ionic and covalent bonding in a compound. If the bonding is strongly ionic, there is little mixing of states from one atom into the states of the others. The decomposed state density will be very dissimilar on the two sites in a binary compound. If the bonding is primarily covalent, the states of all the atoms are strongly mixed together and one would expect to find that the decomposed state density is similar on all sites.

There are two dominant ingredients to the understanding of the electronic structure of this class of compounds. The first ingredient is the expansion of the transition-metal lattice due to the insertion of the *sp* element, and the second is the interaction between the valence *d* shell on the transition metal with the valence *sp* shell of the light element. The largest contribution to the cohesive energy of transition metals is due to the formation of a *d* band from the atomic *d* orbitals.[5–7] If the transition-metal atoms are pulled farther apart, the *d*-band width decreases and the *d*-band broadening contribution to the stability of the lattice is diminished. The loss will be greater the larger the lattice expansion and the larger the extent of the *d* bonding. (The *d* bonding varies quadratically with *d*-band filling and is therefore greatest in the middle of each transition series.)

The second dominant ingredient is the covalent hybridization of atomic states. When two atoms are brought together, their states hybridize with one another to form bonding and antibonding hybrids.[8] This is the familiar interaction that leads to molecular bonding and to band broadening and bonding in solids. When one forms a compound from a transition metal and a light element with a valence *p* shell, the *d* states of the transition metal hybridize with the *p* states to form a bonding hybrid which is more tightly bound than either of the states from which it is formed, and also a band of antibonding states is formed. For most simple crystal structures not all of the *d* states will have the correct symmetry to form hybrids. This leads to nonbonding states in the compound whose energies are close to the energy of the *d* band in the element.

Figure 1 displays the range of electronic structures in this set of transition-metal compounds. The figure contains characteristic features of the states in the compounds PdLi, PdB, and PdF which span the range of behavior found for this class of compounds. The upper half of the figure shows the energy range in which the valence states of the constituent elements are available for interatomic bonding (the energy range in which the logarithmic derivative of the corresponding radial wave function at the atomic sphere is negative). The range for the *d* band of palladium is shown to the left of the vertical energy axis, and that for the *s* and *p* bands of the Li-row element is shown to the right of the axis. As one progresses across the row from lithium to boron to fluorine the valence bands of the light element are progressively more tightly bound. The *s* and *p* valence shells of lithium lie *above* the *d* band of palladium, the *s* and *p* bands of boron are *degenerate* with the palladium *d* band, and both the *s* and *p* band of fluorine lie *below* the palladium valence band. The changes in valence-band width across the Li row reflect the changes in equilibrium volume. As a valence shell (the *p* shell in this case) is filled, the equilibrium volume first decreases because bond-

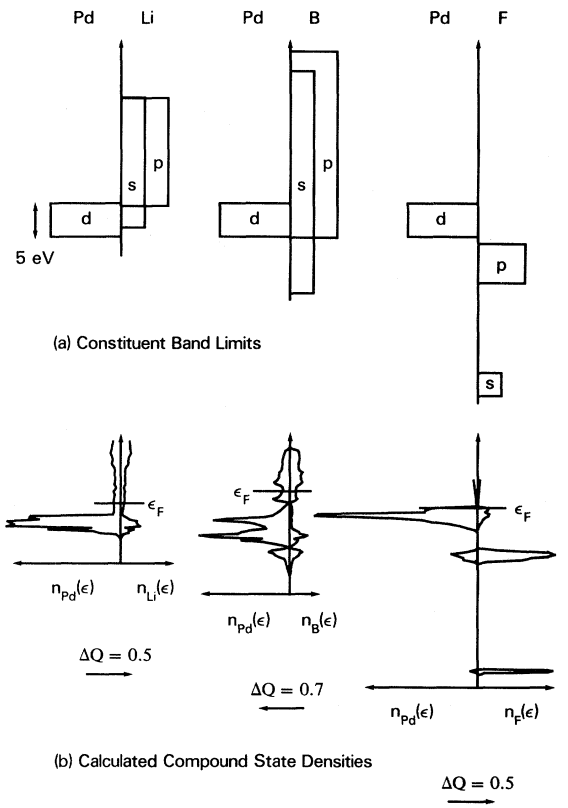

FIG. 1. Dependence of the electronic structure of compounds (b) on the energy positions and widths of the valence states of the constituents (a). The compounds PdLi, PdB, and PdF provide examples in which the valence states of the nontransition metal lie above (Li), near (B), and below (F) the energy of the transition-metal *d* states. Only when the valence states of the constituents are approximately degenerate, does a strong covalent hybridization occur. The rectangular regions in the upper portion of the figure do not represent state densities, they indicate only the energy range in which the constituent atomic states are available for bonding (the energy range in which the logarithmic derivative of the radial wave function is negative on the Wigner-Seitz sphere).

ing states are being filled, then increases as the antibonding states are filled. This leads to a minimum in the volume near a half-filled shell. Thus the volumes of both lithium and fluorine are much larger than that of boron. Since bandwidths reflect the degree of orbital overlap, the valence bands of boron are broader than those of lithium or fluorine. (The constituent band positions and widths were evaluated for the fcc lattice; similar results would be obtained for any close-packed structure.)

The degree of degeneracy between the palladium *d* band and the light-element valence bands is reflected in the strength of the hybridization (interaction) between them as shown in the lower half of Fig. 1. Here, for each of the three compounds, is plotted the electronic density of states in the compound decomposed by site. The density of states on the palladium sites is plotted to the left of the vertical energy axis and the density of states on the light element site is plotted to the right. The energy scale is the same as in the top half of the figure.

Consider first the situation in PdLi. The density of states on the palladium site looks qualitatively like that in pure palladium, with one obvious difference—the *d* band is significantly narrower in the compound than that of elemental palladium shown in the top half of the figure. This decrease in *d*-band width is the result of lattice expansion required for the insertion of the interstitial lithium atoms into the palladium lattice. Since the width of a pure *d* band scales approximately as the inverse of the fifth power of the atomic separation,[9] and the calculated equilibrium separation in PdLi is 22% larger than that calculated for pure Pd, one expects and finds a *d* band that is significantly narrower than that of pure Pd. (Note that the rocksalt structure maintains the fcc Pd-Pd coordination.) Since the lithium valence levels are significantly less tightly bound than the palladium *d* band, there is relatively little interaction between them. This is reflected in the density of states on the lithium site which is seen to be essentially a copy of the palladium density of states. (The small replica of the Pd state density seen in the Li-site state density does not represent a bond, but rather the "tails" of the palladium *d* states passively overlapping onto the Li sites.)

The situation in PdF, on the right-hand side of the figure, is similar. In this case the fluorine *s* and *p* bands are more tightly bound than the palladium *d* band again leading to relatively little interaction. One can clearly see the fluorine 2*s* and 2*p* bands with relatively little amplitude on the palladium sites, and the palladium 4*d* band with little amplitude on the fluorine sites. The existence of energetically separated atomiclike states is characteristic of ionic compounds. The nature of the charge transfer in this system is discussed later. The lattice expansion relative to elemental palladium is somewhat less than that in PdLi, and the *d*-band narrowing is correspondingly less noticeable.

The electronic states in PdB, shown in the center of the figure, are qualitatively different. As shown in the top half of the figure, the boron *s* and *p* bands are more nearly degenerate with the palladium *d* band. The lower half of the figure shows that, as a result, the degree of hybridization between them is correspondingly greater. The boron 2*s* band is sufficiently tightly bound that one sees an identifiable *s* band, but the palladium-*d*-band—boron-*p*-band complex is strongly mixed. One can see the bonding and antibonding states at the bottom and top of the *p*-*d* complex, and the nonbonding *d* states (the palladium-site peak with no mirror peak on the boron site) in between. The overall bonding-antibonding complex is much broader than the *d* band in either PdLi or in pure Pd. PdB is a clear example of what is often called covalent bonding. The atomic orbitals of the constituents are so strongly mixed that the states in the compounds can only be described in terms of the hybrid orbitals.

One is frequently interested in defining the degree

TABLE I. Elemental volumes and bulk moduli, with volumes in cubic bohr radii and bulk moduli in kbar.

Atom	Volume	Bulk modulus	Atom	Volume	Bulk modulus	Atom	Volume	Bulk modulus
Li	128.9	140	Mg	147.7	400	Y	204.7	400
Be	51.3	1300	Al	109.3	900	Zr	150.9	800
B	39.2	3000	Si	96.6	900	Nb	125.4	1600
C	46.6	2100	P	96.3	1100	Mo	108.2	2300
N	48.0	2300				Tc	99.0	3100
O	49.6	1900				Ru	95.1	3200
F	60.3	700				Rh	96.3	2100
						Pd	103.3	1900
						Ag	117.9	1100

TABLE II. Percent deviation of compound volumes from Vegard's law.

	Y	Zr	Nb	Mo	Tc	Ru	Rh	Pd	Ag
Li	+12	+9	−1	−10	−17	−20	−22	−19	−7
Be	+11	+12	+6	+3	+2	+2	+1	+3	+9
B	−3	+1	0	+1	+3	+3	+2	+3	+6
C	−13	−11	−10	−8	−6	−6	−6	−6	−3
N	−22	−18	−15	−11	−8	−7	−9	−8	−9
O	−26	−18	−13	−9	−6	−4	−5	−5	−7
F	−18	−11	−6	−4	+2	+4	+5	+4	+6

of charge transfer in systems such as these. The figure contains examples of two methods used to define the charge transfer, and a comparison of the answer given by the two methods provides an example of why the definition of charge transfer is frequently such a controversial topic. The Fermi level in the compound is indicated in each of the compound state-density plots. In addition, at the bottom of the figure the change in the integrated charge contained in the palladium atomic sphere[10] is printed with an arrow indicating the direction of flow of integrated charge. (For information used for atomic partitioning[10] in this regard, see Tables I and II.)

Consider first the PdLi system. In pure Pd the *d* band is not completely filled, and the Fermi level lies on a peak in the density of states just below the top of the *d* band. In PdLi the Fermi level is seen to lie above the top of the *d* band. If one defines charge transfer by asking whether the palladium *d* band has been filled, the answer for this compound is that the lithium atoms have donated charge to the palladium bands and this is an ionic compound with charge flowing from the electropositive lithium to the relatively electronegative palladium. On the other hand, if one actually integrates charge densities to find the number of electrons contained in the palladium atomic sphere, one finds approximately 0.5 *fewer* electrons in the palladium sphere in the compound than in pure Pd. Yet another way in which to quantify charge transfer is to monitor only changes in the integrated charge associated with localized states, such as the transition-metal *d* states. Because localized states, by definition, have little amplitude in the interstitial region between the atoms, the assignment of charge to them is less affected by the arbitrary partitioning of space into atoms than is the assignment of the entire charge to atoms. According to this accounting scheme, on going from pure Pd to the compound PdLi, Pd gains 0.1 *d* electron.

In the PdB case, the band-filling definition is difficult to apply since the state density is so dissimilar to that in pure Pd. The charge-transfer definition based on integrated charges indicates that boron donates electrons to palladium, as one might expect from simple state-mixing arguments. If one forms hybrids from nondegenerate states, the bonding hybrids have larger amplitude on the atoms with the more tightly bound orbitals while the antibonding hybrids are concentrated on the atoms with less tightly bound orbitals. If the Fermi level lies below the top of the complex, more bonding states are filled than antibonding states, and one expects to find charge transferred to the atoms with more tightly bound orbitals, that is, from boron to palladium in this case.

In PdF the two definitions of charge transfer are seen to give the same direction of charge flow. Since one palladium electron can be used to fill the hole in the fluorine *p* band, the Fermi level in the compound lies deeper below the top of the *d* band than it does in pure Pd. One demonstration of this (not shown in the figure) is that, in NaCl-structure AgF, the Fermi level lies right at the top of the *d* band rather than 4 eV above the *d* band, as it does in pure Ag. The drop in Fermi level for PdF indicates charge flow from palladium to fluorine. Integrating charges also indicates charge flow in this direction. The calculations for PdF exhibit another interesting phenomenon which tends to frustrate efforts to quantify the charge-transfer concept. Despite the change in position of the Fermi level in the *d* bands of Pd upon going from pure Pd to PdF, the number of *d* electrons on Pd in the two systems remains unchanged at 8.8. The mechanism responsible for this paradoxical behavior is hybridization of the *d* band with other states. That is, the *d* band of PdF contains slightly more states than that of pure Pd because of reduced hybridization.[11] The reduced hybridization is consistent with the transfer of non-*d* electrons from the Pd to F, and with the brief discussion of AgF above.

The conflicting views of charge transfer provided by the two definitions underscore the impossibility of defining a single number that will characterize charge transfer in a compound. The question "what is the charge transfer?" can only be answered by choosing some measurable (or calculable) quantity as

the definition of charge transfer. Different definitions will lead to different qualitative and quantitative pictures of the charge transfer. Furthermore, as indicated in the next section, we have not found charge transfer to be a particularly useful concept in trying to understand the chemical trends of the bonding in these materials (despite the fact that the bonding of transition metals to strongly electronegative elements, such as fluorine, is largely ionic[12]).

III. HEATS OF FORMATION

Next, consider the systematics of the heats of formation[13] of the present class of compounds. The same two effects that dominate the electronic structure also determine the qualitative features of the heat of formation. By inserting the *s-p* element into the transition-metal lattice, the *d* band is narrowed, and thus the *d*-band-broadening contribution to the cohesive energy, which dominates the transition-metal cohesive energy, is reduced. The loss of *d*-bond energy is roughly proportional to the volume of the non-transition-metal constituent and to the strength of the *d* bonding in the transition-metal constituent. Therefore, when considering compounds with a fixed Li-row element, the loss varies parabolically across the transition-metal row with its maximum near the center of the row. When considering compounds with a fixed transition metal, the loss is again roughly parabolic with maxima for lithium and fluorine and a minimum for elements with a nearly-half-filled *p* shell.

The hybridization between the *d* band of the transition metal and the *s* and *p* bands of the *s-p* element lead to *sp*—*d* bonding and antibonding hybrids, and to nonbonding *d* states. As is the case for the bonding energy of a diatomic molecule, filling bonding orbitals increases the bond strength, filling nonbonding orbitals has little effect, and filling antibonding orbitals reduces the bond strength. Thus hybridization leads to a term in the heat of formation for compounds of a fixed *s-p* element with the transition metals that becomes more bonding as the bonding hybrids are filled, remains flat as the nonbonding states are filled, and becomes rapidly less bonding as the antibonding states are filled.

In Fig. 2 this picture is developed for compounds formed between boron and the 4*d* transition metals. At the top of the figure is the calculated electronic density of states for a member of this family, PdB, with the bonding, nonbonding, and antibonding features identified. Also indicated is the number of electrons per unit cell needed to fill the bonding states (8 electrons per unit cell) and to fill the nonbonding states (12 electrons per unit cell).

In the lower half of the figure are plotted

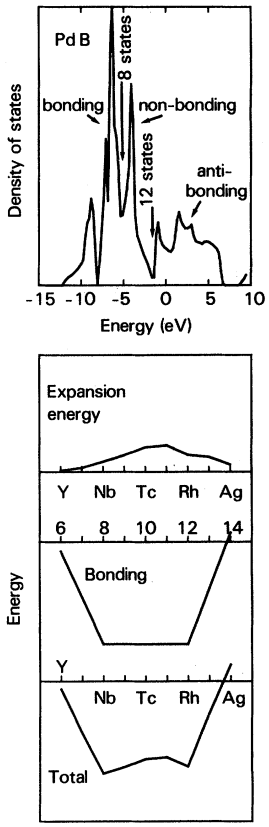

FIG. 2. State density (top panel) and competing contributions to the heat of formation (lower three panels) for systems exhibiting covalent bonding. The expansion energy describes the weakening of the transition-metal bonds by the lattice dilatation required for the accommodation of the non-transition metal. The variation of the expansion energy with transition-metal host reflects the variation of *d*-bond energy across the transition series. (The midseries transition metals have more *d*-bond energy to lose, when the nontransition metal is inserted into the lattice.) The *p*—*d*-bond energy (center portion of lower half of figure) is seen to increase, as the bonding states are filled, to remain constant as the nonbonding states are filled, and to decrease as the antibonding states are filled. (The state density displayed is that for PdB, but those for the transition-metal bromides are similar.) The curve labeled "total" shows the net result. The decomposition of the heat of formation is schematic.

schematic representations of the two components of the heat of formation outlined above. The topmost curve in the panel is the energy cost of expanding the transition-metal lattice to insert the boron atom for each of the 4*d* elements. The cost is proportional to elastic energy of expanding the transition-metal lattice by the volume of boron. The second curve describes the energy gained by forming the *p-d* hybrid. The horizontal axis is the number of elec-

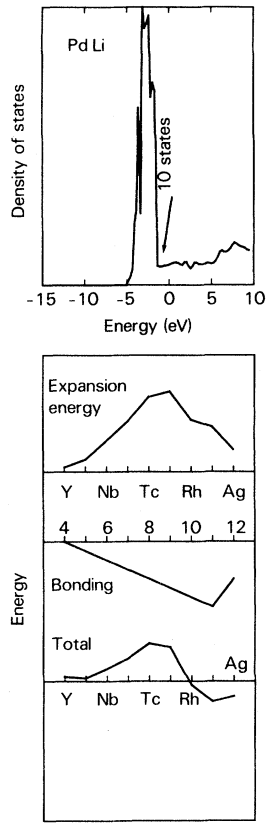

FIG. 3. State density (top panel) and competing contributions to the heat of formation (lower three panels) for systems which do not exhibit strong covalent bonding. The expansion energy describes the weakening of the transition-metal bonds by the lattice dilatation required for the accommodation of the nontransition metal. The variation of the expansion energy with transition-metal host reflects the variation of d-bond energy across the transition series. (The midseries transition metals have more d-bond energy to lose, when the nontransition metal is inserted into the lattice.) The $p-d$-bond energy for the lithium compounds (center portion of lower half of figure) is weaker than that for the boron compounds (Fig. 2). (The state density displayed is that for PdLi, but those for the other transition-metal compounds with lithium are similar.) The curve labeled "total" shows the net result. The decomposition of the heat of formation is schematic.

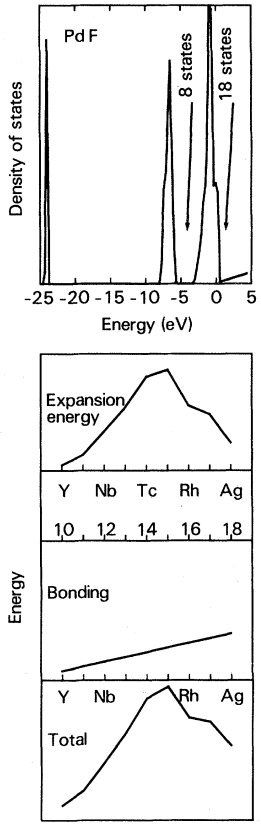

FIG. 4. State density (top panel) and competing contributions to the heat of formation (lower three panels) for systems in which the p states of the nontransition metal lie lower in energy than the d states of the transition metal. The expansion energy describes the weakening of the transition-metal bonds by the lattice dilatation required for the accommodation of the nontransition metal. The variation of the expansion energy with transition-metal host reflects the variation of d-bond energy across the transition series. (The midseries transition metals have more d-bond energy to lose, when the nontransition metal is inserted into the lattice.) The $p-d$-bond energy for the fluorine compounds (center portion of lower half of figure) exhibits no structure, because the Fermi energy lies in the right-most peak of the state density (top portion of figure) for the entire sequence of compounds considered. (The state density displayed is that for PdF, but those for the other transition-metal compounds with fluorine are similar.) The curve labeled "total" shows the net result. The decomposition of the heat of formation is schematic.

trons per unit cell. Since yttrium has three valence electrons as does boron, YB has 6 electrons per unit cell. The bond strength increases up to NbB where all eight bonding states are filled; it is constant during the filling of the nonbonding states up to RhB with 12 electrons per unit cell, then it decreases as the antibonding states are filled. The bottom curve is the sum of the two schematic components. Since the boron volume is relatively small, the sum is dominated by the hybrid-formation term. The expansion energy is evident only in the slight hump for the compounds MoB through RuB.

The situation for PdLi is quite different as shown in Fig. 3. Since lithium has a much larger volume than boron, the volume-expansion term is significantly larger for PdLi than for PdB. Since there is

little hybridization between the palladium *d* band and the lithium valence *s* and *p* bands, the hybridization term is relatively small. The heat of formation is thus dominated by the expansion energy and shows the parabolic dependence across the 4*d* row characteristic of the 4*d* cohesive energies.

Figure 4 shows the corresponding picture for the fluorine compounds. The state density of PdF consists essentially of independent fluorine *s* and *p* states and palladium *d* states. The *p* states are filled at a total of 8 electrons per unit cell, the transition-metal *d* states at 18 electrons per unit cell. Fluorine is also quite a bit larger than boron so the volume-change term in the fluorine compounds is large as shown in the top curve in the lower panel of the figure. Both the fluorine *p* band and the transition-metal *d* band are essentially nonbonding since they are well separated in energy. There is a net bond due to the transfer of an electron from the transition metal to fill the hole in the fluorine *p* band, but little chemical structure in the hybridization curve. The trend of the heat of formation is again dominated by the volume-change term.

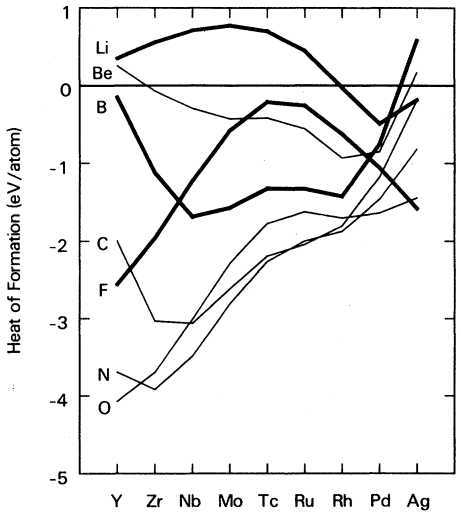

FIG. 5. Variation of heat of formation with number of valence electrons. These nonschematic theoretical results for the Li-row compounds (NaCl structure) exhibit the fundamental valence-electron-count dependencies presented and analyzed schematically in Figs. 2, 3, and 4. The 63 heats of formation shown here were obtained from direct subtraction of total energies calculated for the compounds and their constituents. The total energies were obtained using self-consistent energy-band calculations based on the "local-density" treatment of electronic exchange, and correlation and the augmented-spherical-wave procedure for the solution of the effective-single-particle equations. The lattice constants of the compounds and the elements were obtained by minimization of the calculated total energy.

The heat-of-formation trends developed schematically in Fig. 2 are confirmed by the results of the detailed self-consistent electronic-structure and total-energy calculations, as shown in Fig. 5. The calculated heats of formation for all of the NaCl-structure[14] compounds formed between a Li-row element and the 4*d* metals are plotted as a function of the transition metal. The calculated curves for lithium, boron, and fluorine with the 4*d* series are highlighted. One can see the progression of behavior from the lithium compounds with a large repulsive volume contribution and little hybridization through the boron compounds to the carbides, nitrides, and oxides, which have a larger bonding contribution since their *p* states are more nearly degenerate with the transition-metal *d* bands, to fluorine which has an essentially constant bonding term and a larger volume-change cost.

As explained above, the structure in the boron curve is related to filling of bonding and antibonding states. Since different Li-row elements have a different number of valence electrons, features that occur at a fixed number of electrons per unit cell will be observed for different transition metals when the Li-row element is changed. For example, when there are well-defined hybridized states, the bonding *p-d* hybrid is filled at 8 electrons per unit cell. This produces a minimum in the heat of formation for systems with eight electrons per unit cell, such as MoBe, NbB, and ZrC. Similarly, the antibonding states begin to fill at 12 electrons per unit cell in compounds with the well-defined hybrids, and one finds structure in the heat-of-formation curve for these systems (PdBe, RhB, and RuC).

The fact that structure in the heat of formation is not always found for compounds with 8 or 12 electrons per unit cell is a demonstration that a rigid-band model is not appropriate either for all compounds formed from a fixed Li-row element and the 4*d* metals, or for compounds formed from a fixed 4*d* metal and the Li-row. The second of these conclusions was evident from the densities of states plotted in Fig. 1: The density of states of PdF bears little resemblance to that of PdLi. The rigid-band model is somewhat more appropriate when the light element is held fixed and a series of transition metals considered. The degree of *p-d* hybridization depends on the relative energies of the transition-metal *d* band and the *sp* band of the Li-row element. As one progresses across the 4*d* series, the *d* band becomes more tightly bound, but the change is only about 5 eV rather than the tens of volts difference between the center of gravity of the *p* band in Li and that in F.

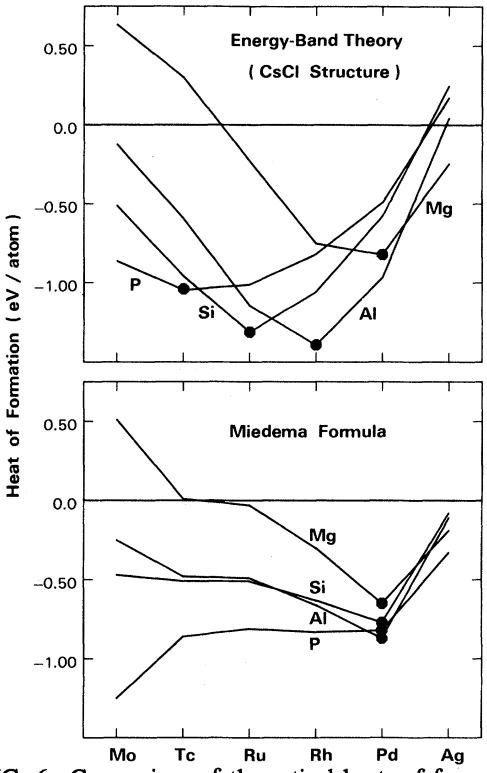

FIG. 6. Comparison of theoretical heats of formation with those given by Miedema's empirical formula. Dots indicate the most-strongly-bound member of each compound sequence (except for the P curve in the Miedema panel where it marks the break in the curve). The progression of the dots from right to left as the valence of the nontransition metal is increased is a direct consequence of the filling of the p–d covalent-bond states (see Figs. 2–4). The fact that Miedema's results do not exhibit this progression indicates that Miedema's formula is based on a physical model different from that given by our energy-band calculations (Figs. 2–4). Note, however, the general agreement between the two sets of results. The available measurements relevant to this figure are

$$\Delta H(\mathrm{AlAg}) = -0.04,\quad \Delta H(\mathrm{AlPd}) = -0.96\ ,$$

$$\Delta G(\mathrm{Al_{0.6}Zr_{0.4}}) = -0.55,\quad \Delta G(\mathrm{Al_{0.43}Zr_{0.57}}) = -0.45\ ,$$

$$\Delta H(\mathrm{AlY}) = -0.91,\quad \Delta H(\mathrm{MgAg}) = -0.19\ ,$$

$$\Delta H(\mathrm{MgY}) = -0.13,\quad \Delta H(\mathrm{SiMo}) = -0.43\ ,$$

$$\Delta H(\mathrm{SiZr}) = -0.80,\quad \Delta H(\mathrm{Si_3Nb_5}) = -0.63\ .$$

The AlY value is from Bayanov (Ref. 17); the other data are from Hultgren *et al.* (Ref. 18). Note that when comparing measured and computed values, the standard state of the non-transition-metal elements to which the compound total energy is compared is usually not the same as the fcc metallic state used as a reference in our calculations. Note also, however, that this difference does not affect the variation of the heat of formation with transition-metal partner.

IV. COMPARISON WITH MIEDEMA'S EMPIRICAL THEORY

As a final point, we compare in Fig. 6 the predictions of our energy-band theory with those of Miedema's empirical formula.[15] Figure 6 illustrates two important points. First, our theoretical results are in general agreement with Miedema's, confirming both the relevance of our calculations to real systems and the practical utility of Miedema's formula. Note, in particular, that among the 18 compounds considered in Fig. 6 the only disagreements in the sign of the heat of formation between our calculations and Miedema's are for systems for which the heat of formation is very small. The second important feature of Fig. 6 is the fact that the band-theory results strongly reflect the chemical trends discussed above, whereas the values given by the empirical formula do not. That is, the band-theory results dramatically exhibit just the dependence on the total number of valence electrons per cell that one would expect on the basis of the covalent-bond state density shown in Fig. 2. We see that the most strongly bound member of each of the compound sequences (the dot) shown in Fig. 6 is the one for which the electron count of 12 permits all the bonding levels (see Fig. 2) to be filled and all the antibonding levels to be left empty. The result is the progression of most-strongly-bound compound (the dots) from left to right in Fig. 6, as the transition-metal constituent balances the valence decrease in going from P to Si to Al to Mg. The state density of Fig. 2 and the interpretation it provides of Fig. 6 emphasize properties of the compound over those of the constituents. Miedema's formula and the microscopic picture on which it is based both do the opposite: They emphasize properties of the constituents. It is not surprising, therefore, that the empirical formula fails to describe the covalent-bonding trend shown in Fig. 6. Our view is, therefore, similar to that expressed in Williams *et al.*[16] and can be summarized by saying that Miedema's formula is an immensely useful predictor of compound behavior; our only known disagreements with its predictions are quantitative details, which seldom affect the sign of the heat of formation, but strongly affect the plausibility of the microscopic picture in terms of which the formula is usually described.

V. CONCLUSION

We have carried out a series of detailed calculations of the electronic structure of a class of metallic compounds. From these calculations we have abstracted the two dominant effects that describe both the electronic density of states and the chemis-

try of the compound heats of formation: (1) The increased transition-metal—to—transition-metal distance resulting from the insertion of the light element into the lattice, and (2) the hybridization between the *d* states of the transition metal and the *sp* states of the Li-row element.

[1]V. Ern and A. C. Switendick, Phys. Rev. 137, A1927 (1965).

[2]A. Neckel, P. Rastl, R. Eibler, P. Weinberger, and K. Schwarz, J. Phys. C 9, 579 (1976).

[3]O. K. Andersen, H. L. Skriver, H. Nohl, and B. Johansson, Pure Appl. Chem. 52, 93 (1980).

[4]A. R. Williams, J. Kübler, and C. D. Gelatt, Jr., Phys. Rev. B 19, 6096 (1979).

[5]J. Friedel, in *The Physics of Metals,* edited by J. M. Ziman (Cambridge University Press, London, 1969), Chap. 8.

[6]C. D. Gelatt, Jr., H. Ehrenreich, and R. E. Watson, Phys. Rev. B 15, 1613 (1977).

[7]D. G. Pettifor, J. Phys. F 8, 219 (1978).

[8]J. B. Goodenough, *Magnetism and the Chemical Bond* (Interscience, New York, 1963).

[9]V. Heine, Phys. Rev. 153, 673 (1967).

[10]Note that, while the size of the *unit* cell is determined by minimization of the total energy, the subdivision of the unit cell into *atomic* cells requires an additional criterion. For systems obeying Vegard's law (unit-cell volume equals the sum of elemental atomic-cell volumes) the atomic cells of the compound are taken to be those of the elements. When there is a deviation from Vegard's law, the volume *difference* is allotted to the atomic spheres according to the following prescription, $\delta\Omega_1/\delta\Omega_2 = (B_2/B_1)(\Omega_1/\Omega_2)$, where B and Ω refer to the calculated bulk modulus and volume of the constituent elements. This prescription can be thought of as "preparing" the elements so that Vegard's law will be perfectly obeyed. The relative amount of expansion or compression performed on each constituent is determined by minimizing the elastic energy of the preparation step. We emphasize that the preparation step is only a physical interpretation of our subdivision of the compound unit cell into atomic cells; the calculated heats of formation refer to elements at their equilibrium volumes.

[11]A single band always contains two (spin-up and spin-down) electrons per unit cell. The interesting difference between pure Pd and the compound PdF is that the presence of the fluorine in the compound displaces the *s* states of Pd from the energy region of the Pd *d* states. The result is that there is less mixing (hybridization) of the Pd *s* and *d* states in the compound, giving what we call the "*d* states" a more purely *d* character. Note that the increased *d*-band "purity" is consistent with the Fermi level lying lower in the *d* bands of the compound, despite the absence of significant *d*-electron charge transfer.

[12]J. C. Phillips, J. Phys. Chem. Solids, 34, 1051 (1973).

[13]The heat of formation is the difference between the total energy of a unit cell of the compound and the sum of the energies of the constituents in their standard states. For purposes of the present calculations the standard state for all elements is taken to be a metallic fcc crystal.

[14]We report here our results calculated for the NaCl crystal structure, because, of the crystal structures our computer programs can treat (CuAu, CsCl, and NaCl), the NaCl structure is the most appropriate to compounds in which the constituents differ significantly in size. That is, the NaCl is a particularly close-packed structure for binary compounds whose constituents differ significantly in size. We have calculated the heat of formation for the same set of 63 compounds considered in Fig. 5 using the CsCl structure; while the magnitudes of the heats of formation differ somewhat, the chemical trends are extremely similar.

[15]A. R. Miedema and P. de Chatel in *Theory of Alloy Phase Formation,* edited by L. H. Bennett (American Institute of Metallurgical Engineers, New York, 1980); Data for P from A. R. Miedema (private communication).

[16]A. R. Williams, C. D. Gelatt, Jr., and V. L. Moruzzi, Phys. Rev. Lett. 44, 429 (1980).

[17]R. Bayanov, J. Phys. Chem. 45, 1077 (1971).

[18]R. Hultgren, R. L. Orr, and K. K. Kelley, *Selected Values of Thermodynamic Properties of Metals* (Wiley, New York, 1963).